European Polymer Journal 46 (2010) 1049–1062

Contents lists available at ScienceDirect

European Polymer Journal

journal homepage: www.elsevier.com/locate/europolj

Viscoelastic and dielectric behaviour of thin films made from siloxane-containing poly(oxadiazole-imide)s

Mariana-Dana Damaceanu *, Valentina-Elena Musteata, Mariana Cristea, Maria Bruma

"Petru Poni" Institute of Macromolecular Chemistry, Aleea Gr. Ghica Voda 41A, Iasi-700487, Romania

ARTICLE INFO

Article history:
Received 11 December 2009
Received in revised form 20 January 2010
Accepted 20 January 2010
Available online 28 January 2010

Keywords:
Dielectric properties
Poly(oxadiazole-imide)s
Relaxation
Tensile properties
Viscoelastic properties

ABSTRACT

Siloxane-containing poly(oxadiazole-imide)s were prepared by polycondensation reaction of two aromatic diamino-oxadiazoles with a dianhydride containing tetramethylsiloxane moiety. Free-standing flexible films having good mechanical properties were made therefrom. The polyimides exhibited high thermal stability with initial decomposition temperature being above 440 °C and glass transition in the range of 165–183 °C. The dielectric constant values, measured at room temperature and in the frequency domain of 1 Hz–1 MHz, are in the range of 2.69–2.90, being significantly lower in comparison with that of **Kapton HN**® film, whose dielectric constant values ranged from 3.13 to 3.24. The dielectric loss values are low, in the same range with those of **Kapton HN**®. The dielectric spectroscopy data corroborated with the dynamo-mechanical analysis ones showed distinct sub-glass transitions for these polymers: γ relaxations with activation energies of 44 and 45 kJ/mol, and a β relaxation with an activation energy of 107 kJ/mol. The dielectric properties are discussed in comparison with those of **Kapton HN**® film measured under the same conditions.

1. Introduction

Aromatic polyimides possess many useful properties, such as excellent dimensional stability, low dielectric constant, high glass transition temperature and outstanding thermal and thermooxidative stability. Therefore, they are widely used as interlayer dielectrics, flexible circuitry substrates, stress buffers, and passivation layers, owing to their relatively low dielectric constant. Low dielectric constant and low interfacial stress are desirable for high performance devices with good reliability. Since the square root of the dielectric constant is inversely proportional to the signal propagation speed, a low dielectric constant material allows for faster signal propagation speed with less attenuation. Thus, the dielectric properties of the material play an important role in the performance of the device. It is well-known that a successful dielectric material must have reasonably good electrical properties, including dielectric constant, dielectric loss, and breakdown voltage. The dielectric constant is frequency dependent and is composed of electronic, atomic, and dipole orientational contributions. The dielectric constant relates to the polarizability of a material and is therefore strongly dependent on chemical structure. The dielectric permittivity of a material is, in general, a complex quantity, when measured in the frequency domain. Its real part (ε') is called the "dielectric constant" and decreases with increasing frequency with characteristic steps. Its imaginary part (ε'') is usually called the "dielectric loss" and may show the maxima on the diagrams versus frequency (or versus temperature). Both are related to ε_0 the permittivity of the free space (equal to 8.85×10^{-12} F m^{-1}). The dielectric loss is a measure of the energy required for molecular motion, that is the energy dissipated in this motion in the presence of an electric field. It consists of two contributions: energy losses due to the orientation of molecular dipoles, and energy losses due to the conduction of ionic species [1–6]. Materials that possess low dielectric constants (low-k) are being developed to replace silicon

* Corresponding author. Fax: +40 232 211299.
E-mail address: damaceanu@icmpp.ro (M.-D. Damaceanu).

0014-3057/$ - see front matter © 2010 Elsevier Ltd. All rights reserved.
doi:10.1016/j.eurpolymj.2010.01.020

dioxide (SiO_2, $k = 3.5$) as the inter-level dielectric. Recently, the specifications for insulating films are that their dielectric constants should be ca. 3.0 and, within the next generation of integrated circuit production, devices may require for materials to have dielectric constants approaching or below 2.0. A low dielectric constant is one of the most attractive properties of polyimide materials for microelectronics applications. In order to achieve a polymer structure with a low dielectric constant, repeating units with low polarity and low polarizability are needed [7,8]. For example, the use of nonpolar monomers containing dimethylsiloxane moieties leads to polyimide systems with lower dielectric constant than classical aromatic polyimides. Moreover, the presence of the siloxane components in the structure of polyimides allows for increased impact resistance, excellent adhesion, gas permeability and reduced water absorption, while maintaining the thermal and mechanical stability that is adequate for most microelectronic applications [9–11].

On the other hand, aromatic polymers containing 1,3,4-oxadiazole ring in the main chain are also well-known for their high thermal resistance in oxidative atmosphere, good hydrolytic stability, tough mechanical properties [12–14] and low dielectric constant [15–17]. Poly(arylene-oxadiazole)s, like poly(*p*-phenylene)s and poly(*p*-phenylene-vinylene)s or polythiophenes, give easily redox reactions, chemically or electrochemically, and the resulting conducting materials are good candidates for electrochemical sensors or electroluminescent devices that can be used in data storage, telecommunications and other applications. Some polyoxadiazoles have semiconducting properties, others can be electrochemically doped, thus becoming electroconductors, and other structures have liquid crystalline properties, which enlarge their potential applications in advanced technologies. They exhibit excellent fiber and film-forming capabilities, thus being considered for use as heat-resistant reinforcing fibers for advanced composite materials, highly resistant fabrics for the filtration of hot gases, special membranes for gas separation or reverse osmosis. Polyoxadiazoles could be precursors for highly oriented graphite fiber, films and blocks to be used in construction of electronic instruments based on X-, neutron- or α-rays, or in the construction of nuclear reactor walls [18–22]. As compared with the first years of the poly(1,3,4-oxadiazole)s research (1960–1970), when they were studied for their high thermal stability, in the recent period, the electronic properties combined with their high heat resistance made them attractive for applications in microelectronics, optoelectronics, advanced telecommunications or other related fields. The incorporation of oxadiazole together with imide rings and flexible dimethylsiloxane groups into the polymer chain is expected to provide a good combination of high performance properties and good processability, particularly in thin films and coatings.

This paper is dealing with the study of the mechanical and dielectric properties, as well as other physical processes taking place during heating of thin films made from siloxane-containing poly(oxadiazole-imide)s, by using dynamo-mechanical analysis (DMA) and broad-band dielectric spectroscopy (BDS). The data showing the dielectric properties are discussed in comparison with those obtained for commercial **Kapton HN**® film measured under the same conditions.

2. Experimental

2.1. Monomers

2,5-Bis[4-(*p*-aminophenoxy)-phenylene]-1,3,4-oxadiazole (**Ox1**) and 2,5-bis[3-(*p*-aminophenoxy)-phenylene]-1,3,4-oxadiazole (**Ox2**) were prepared according to previously reported procedures [23–25]. ^{1}H NMR (DMSO-*d*6, 400 MHz, ppm), **Ox1**: 8.00 (d, 4H), 7.02 (d, 4H), 6.85 (d, 4H), 6.67 (d, 4H), 5.09 (s, 4H); **Ox2**: 8.08 (d, 4H), 7.16 (d, 4H), 7.08 (t, 2H), 6.45 (d, 2H), 6.33 (s, 2H), 6.25 (d, 2H), 5.33 (s, 4H).

The dianhydride containing dimethyl-substituted siloxane groups (**I**), namely 1,3-bis(3,4-dicarboxyphenyl)-1,1,3,3-tetramethyldisiloxane anhydride, was prepared by a published multi-step reaction [26]. ^{1}H NMR (DMSO-*d*6, 400 MHz, ppm): 8.15–8.06 (m, 4H), 8.07 (d, 4H), 0.47 (s, 12H).

2.2. Polymers

The polycondensation reactions (scheme 1) was run with equimolar amounts of 1,3-bis(3,4-dicarboxyphenyl)-1,1,3,3-tetramethyldisiloxane anhydride and 2,5-bis[4-(*p*-aminophenoxy)-phenylene]-1,3,4-oxadiazole or 2,5-bis[3-(*p*-aminophenoxy)-phenylene]-1,3,4-oxadiazole in 1-methyl-2-pyrrolodinone (NMP) as solvent, at a concentration of 8–10% total solids and at room temperature for 2 h, followed by heating at 185–195 °C for 3–4 h. The final polyimide solutions were partially poured into water to precipitate the solid polymer, while the rest was poured onto glass plates in order to prepare thin films. The solid polymers were further filtered, washed twice with water and once with ethanol, and dried in oven at 120 °C. They were then used for various studies.

^{1}H NMR spectra of the polyimides **P-1** and **P-2** were recorded in order to confirm the structure of the polymers. Thus, in the aromatic region the polymers exhibited multiplets due to the aromatic protons of phenylene and benzimide rings, as follows: **P-1**: 8.20–7.86 (m, 10H) and 7.56–7.16 (m, 12H), **P-2**: 8.19–7.53 (m, 10H), 7.35–7.21 (m, 12H). In the aliphatic region, all the polymers presented multiple singlets readily distinguished by a 0.01–0.07 ppm shift that can be attributed to the CH_3 protons of dimethylsiloxane units that are present in syn–anti conformations, as follows: **P-1**: 0.48, 0.43, 0.40, 0.35 and 0.28 ppm, **P-2**: 0.45, 0.40, 0.39 and 0.33 ppm.

The structures of the polyimides were identified by FTIR spectra, as well. The absorption bands characteristic for imide ring appeared at 1770–1780 cm^{-1} (asymmetrical C=O imide stretching), 1710–1720 cm^{-1} (symmetrical C=O imide stretching) and 720–740 cm^{-1} (imide ring deformation). It was observed that the broad IR absorption band at 3350–3450 cm^{-1} characteristic of NH amidic and the narrow absorption peak at 1650–1660 cm^{-1} due to C=O group in amide linkage disappeared almost

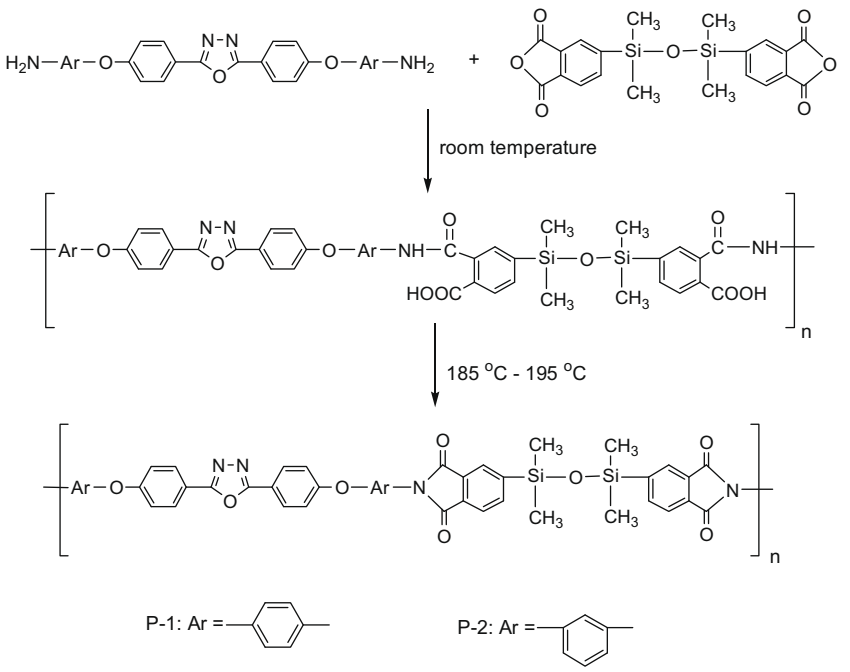

Scheme 1. Synthesis of siloxane-containing poly(oxadiazole-imide)s.

completely. This means that the conversion of the intermediate polyamidic acid into final polyimide structure was quantitative by polycondensation in solution at high temperature. All the spectra showed a peak at 970–960 cm^{-1} and 1020–1010 cm^{-1} characteristic for oxadiazole ring; the siloxane group was evidenced by clear absorption peaks at 1065, 1070 cm^{-1}, while Si–CH_3 groups were evidenced by absorption bands at 1300, 1250 and 795 cm^{-1}. The C–H aliphatic linkage of CH_3 groups showed an absorption peak at 2950 cm^{-1} while the C–H linkage of aromatic rings showed a peak at 3060 cm^{-1}.

2.3. Polymer films

Films of these polymers were prepared by casting a solution of 8–10% concentration of polymers in NMP onto glass plates, followed by gradual heating from room temperature up to 200 °C, and kept at 200 °C for 1 h. Transparent coatings resulted having strong adhesion to the glass support. In order to take these films off the plates it was necessary to put them in hot water for 1–2 h. The resulting free-standing films of these polymers having the thickness in the range of 40–90 μm were flexible, tough and resisted to repeat bending.

The **Kapton HN**® film having the thickness in the range of 120–130 μm was purchased from CS Hyde Company, USA.

2.4. Measurements

^{1}H NMR spectra of the polymers were measured with a BRUKER Avance DRX 400 MHz, by using DMSO-*d*6 and tetramethylsilane (TMS) as standard.

The infrared spectra of the polymers were recorded on FTIR Bruker Vertex 70 Spectrophotometer, using KBr pellets.

Average molecular weights were measured by means of gel permeation chromatography (GPC) using a Waters GPC apparatus, provided with refraction and UV photodiode array detectors and a Shodex column. Measurements were carried out with polymer solutions having 2% concentration, using dimethylformamide (DMF) with $NaNO_3$ (0.1 mol L^{-1}) as solvent and eluent at a rate of 0.6 mL min^{-1}. Polystyrene standards of known molecular weight in a solution of DMF/0.1 mol $NaNO_3$ were used for calibration.

The thermal stability of the polymers was investigated by thermogravimetric analysis (TGA) using a Seiko Robotic RTG 220 thermobalance. Approximately 2–6 mg of a polymer were placed in platinum pans and heated from room temperature to 600 °C at 10 °C/min in air. The temperature of 5% weight loss was considered to be the beginning of decomposition or the initial decomposition temperature (IDT). The maximum decomposition rate temperature, which is the maximum signal in differential thermogravimetry (DTG) curves, was also recorded.

The glass transition temperature (T_g) of the precipitated polymers was determined by using a Seiko Robotic Differential Scanning Calorimeter DSC 6200C. Approximately 3–8 mg of each polymer were crimped in aluminium pans and run in nitrogen with a heat–cool–heat profile from room temperature to 380 °C at 20 °C/min, with 3 min isothermal stabilization times at the temperature extremes. The mid-point temperature of the change in slope of the DSC signal of the second heating cycle was used to determine the glass transition temperature values of the polymers.

Mechanical properties of the polymer films were analysed by tensile testing using a SHIMADZU EZ TEST, 5 KN. The samples were used in the form of strips having the thickness of 0.04–0.09 mm, gauge length of 35 mm and width of 4 mm. Stiffness, tensile strength and elongation-at-break were determined at 50 mm/min cross-head speed. The tensile stress (MPa) versus tensile strain (%) dependencies was recorded.

Dynamic mechanical analysis (DMA) was performed with a Perkin Elmer Diamond apparatus equipped with a standard tension attachment. The experiments were run on film samples with dimensions $10 \times 10 \times 0.04$ mm by heating from -150 °C up to beyond the temperature of the glass transition, with the heating rate of 2 °C/min. The film samples were longitudinally deformed by a small sinusoidal stress at a frequency of 1 Hz and the resulting strain was measured. The variations of the storage modulus E', loss modulus E'' and tension loss tangent tan δ ($\tan \delta = E''/E'$) as functions of temperature were obtained.

Dielectric spectroscopy measurements of the polymer films at various temperatures in the range of 173–423 K and in the frequency range of 10^{-1}–10^{6} Hz have been performed using a Novocontrol Dielectric Spectrometer (GmbH Germany), CONCEPT 40. Polymer films were placed in a flat parallel plate capacitor arrangement having gold plated electrodes with 20 mm diameter. The thickness of the films was in the range of 0.04–0.07 mm. The amplitude of AC applied voltage was 1 V.

3. Results and discussion

The poly(oxadiazole-imide)s **P-1** and **P-2** studied here are based on a dianhydride containing dimethyl-substituted siloxane group and two aromatic diamines containing oxadiazole ring. These polyimides have been prepared by polycondensation reaction of equimolar amounts of siloxane-containing dianhydride with a diamino-oxadiazole in NMP, which firstly yielded polyamidic acids at room temperature, that after heating at high temperature in solution resulted in the corresponding poly(oxadiazole-imide)s. The resulting polyimide solutions were used partially to cast thin films and partially to isolate the solid polymer by precipitating in water. As it was shown before, the structures of these polyimides were demonstrated by ^{1}H NMR and FTIR spectra. The molecular weight of polyoxadiazole-imides **P-2** was measured by gel permeation chromatography (GPC), by using polystyrene standards. The weight average molecular weight value M_w is 103 000, the number average molecular weight value M_n is 59 000, while the polydispersity M_w/M_n is 1.75. The polyimide **P-1** was not enough soluble at room temperature in DMF for molecular weight measurements. It should be noted that gel permeation chromatography measurements by using polystyrene as standard provide only a crude estimate of molecular weights and not an accurate evaluation. However, the polyimide **P-2** has fairly high values of molecular weight and narrow molecular weight distribution.

The thermal stability of the polymers was investigated by thermogravimetric analysis. These polyimides are highly thermostable, their decomposition starting above 440 °C. As expected, the polyimide **P-1** that contains only *para*-catenation in the diamine segment shows a slightly higher decomposition temperature (450 °C) than the other polyimide, **P-2,** which has some *meta*-catenation (445 °C). The decomposition of the polyimides takes place in two steps as shown by TGA and DTG values of the maximum decomposition temperatures calculated on these curves: at about 500 °C, the first step, and close to 600 °C, the second step. The first maximum was probably due to the destruction of methylene groups, more sensitive to degradation, while the second maximum of the decomposition was due to the degradation of polymer chain itself. These polymers have comparable thermal stability and similar behaviour to degradation with related copoly(oxadiazole-imide)s based on siloxane-containing diamines and other dianhydride [27].

These polyimides do exhibit a glass transition temperature (T_g), in the range of 165–183 °C, as shown by differential scanning calorimetry (DSC). The DSC curves of the siloxane-containing polyimides are displayed in Fig. 1.

Compared with wholly aromatic polyimides which usually do not show glass transition, or their T_g is very high as in the case of **Kapton HN**® film [28], or T_g is practically in the same domain with their decomposition, the present polyimides show relatively low glass transition temperature values. It is believed that the insertion of siloxane units in the polyimide chains leads to a lower T_g. Similar effect was noticed previously [26]. Moreover, the presence of *meta*-catenation in the macromolecular chain of **P-2** is responsible for the reduction with 20 °C of the T_g value as compared to that of **P-1**. For these polyimides it can be noticed that there is a large interval between the glass transition and decomposition temperature which makes these polymers attractive for thermoforming processing.

The tensile properties of the poly(oxadiazole-imide) films **P-1** and **P-2** are collected in table 1.

Elastic modulus, tensile strength and elongation to break have been determined as averages of three drawing experiments. These polymers showed similar type of behaviour with respect to the elastic deformation range at small strains. The values of tensile strength are in the

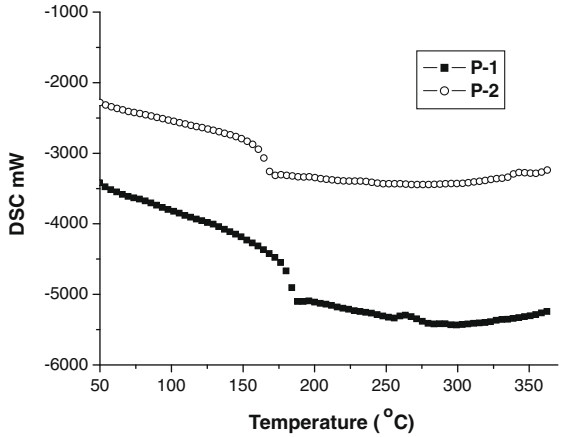

Fig. 1. DSC curves of siloxane-containing polyimides.

Table 1
Tensile properties of siloxane-containing polyimide films.

Polymer	Tensile strength (MPa)	Elastic Modulus (GPa)	Elongation at break (%)
P-1	40	1.89	4.3
P-2	10	1.46	1.5

range of 10–40 MPa, elastic modulus in the range of 1.46–1.89 GPa and elongation at break in the range of 1.5–4.3%. The standard deviation of the tensile strength, elastic modulus and elongation at break values of these polyimides vary within 2.77–8.23 MPa, 0.37–0.54 GPa and 0.13–0.15% range, respectively. As can be seen in Table 1, the mechanical properties of siloxane-containing polyimides are comparable with those of other polyoxadiazoles, e.g. polyoxadiazole-ketones which have tensile strength of 48 MPa, elastic modulus of 1.46 GPa and draw ratio at break of 1.36 [29], indicating that the films prepared from these polymers can be used as advanced materials in moderate conditions.

Electrical insulating properties of the polymer films **P-1** and **P-2** were evaluated on the basis of dielectric constant and dielectric loss and their variation with frequency and temperature. For comparison, the variation of dielectric constant and dielectric loss with frequency and temperature of commercial **Kapton HN**® film, which is one of the most common polyimides used as dielectric in advanced microelectronic applications, were also recorded. The dielectric constant ε' and dielectric loss ε'' of the polymer films **P-1**, **P-2** and **Kapton HN**® are displayed from 10^{-1} to 10^{6} Hz at different temperatures, in the range of −100 to +150 °C. Fig. 2 presents the dependence of real and imaginary part of complex permittivity, on frequency, at three chosen temperatures: −100, +20 and +100 °C.

At very low and moderate temperatures the dielectric constant increases very slowly, linearly, with decreasing of frequency, taking low values even at very low frequency. The dielectric constant of polymers decreased gradually with increasing frequency because the response of the electronic, atomic and dipolar polarizable units varies with frequency in the specific domain. This behaviour can be attributed to the frequency dependence of the polarization mechanism. The magnitude of the dielectric constant is dependent upon the ability of the polarizable units to orient fast enough to keep up with the oscillation of the alternative electric field [30,31]. From Fig. 2 it can be observed that the magnitude of the dielectric constant for siloxane-containing poly(oxadiazole-imide)s **P-1** and **P-2** is lower than that of **Kapton HN**® film; in the same time, the variation of the dielectric constant with frequency for **P-1** and **P-2** films is much lower than for **Kapton HN**® film. All these demonstrate the low capability of polarization of these polymers as compared to **Kapton HN**® film due to the presence of nonpolar siloxane units. An increase of the dielectric constant can be observed for **P-2** and **Kapton HN**®, at high temperature (100 °C) and low frequency due to the mobility of charge carrier. The poly(oxadiazole-imide) **P-1** exhibited low dielectric constant over the entire interval of frequency (10^{-1}–10^{6} Hz), even at 100 °C. For many applications, dielectric materials with stable dielectric constant and dissipation factor values across large frequency and temperature range are highly preferred.

The dielectric constants of the films obtained from polyimides **P-1** and **P-2,** and **Kapton HN**® at 1 Hz, 100 Hz, 1 kHz and 1 MHz, at room temperature (23 °C) are presented in Table 2. The dielectric constant values of the polymers **P-1** and **P-2** at room temperature and in the frequency range of 1 Hz–1 MHz are in the range of 2.69–2.90, and are significantly lower in comparison with that of **Kapton HN**® polyimide film whose dielectric constant values ranged from 3.13 to 3.24. The low dielectric constant values are explained by the presence of flexible tetramethylsiloxane group in the polymer chain which decreased the chain packing and increased the free volume of the polymers, lowering the polarization by decreasing the number of polarizable groups per unit volume and thus decreasing the dielectric constant [32].

At high temperature the dielectric loss increased sharply with decreasing frequency due to the mobility of charge carriers. Similar behaviour was observed in the case of poly(phenylquinoxaline-imide) films [33]. At 100 °C, the dielectric loss for **P-1, P-2** and **Kapton HN**® is almost invariable in the range of 10 Hz–1 MHz; at low frequency (0.1–10 Hz) **P-2** and **Kapton HN**® films exhibited higher dielectric loss when compared with that of polymer **P-1**, in the same conditions. This can be explained by the presence of a higher concentration of dipoles in the case of **P-2** and **Kapton HN**®, when compared with **P-1**. At moderate temperature the dielectric loss exhibited low values in the interval of measured frequency for siloxane-containing poly(oxadiazole-imide)s **P-1** and **P-2**, while for **Kapton HN**® film the dielectric loss increases sharply at high frequency (1 kHz–1 MHz). At very low temperature the **P-2** presents a constant dielectric loss on the whole range of measured frequency, while **P-1** and **Kapton HN**® show an increase of dielectric loss with a maximum centred at 10 Hz. The dielectric loss values of the studied films at 1 Hz, 100 Hz, 1 kHz and 1 MHz and room temperature (23 °C) are collected in Table 2. **P-1** and **P-2** films present low values of dielectric loss, comparable with that of **Kapton HN**®. Low values of the dielectric loss are indicative of minimal conversion of electrical energy into heat in the dielectric material. It is advantageous to have low values for both dielectric constant and dielectric loss because the electrical signals loss will be lower in the dielectric medium.

Generally, polymers possess relaxation processes that are obviously determinants of the physical properties of the materials made from them [34]. Essentially, all amorphous polymers possess at least two relaxation processes. One of these processes is the glass transition, often designated as the "α" relaxation. Up to the glass transition temperature, at least one additional relaxation process can be found. Such sub-glass or secondary process, often designated as the "β" relaxation, is extremely broad, so much that it has proven difficult to arrive at a definitive shape description. Such relaxations are often "complex" in the sense that they can show evidence of poorly resolved overlapping components. A sub-glass or secondary process could be assigned to cooperative conformational transitions involving nearby bonds that allow local conformational

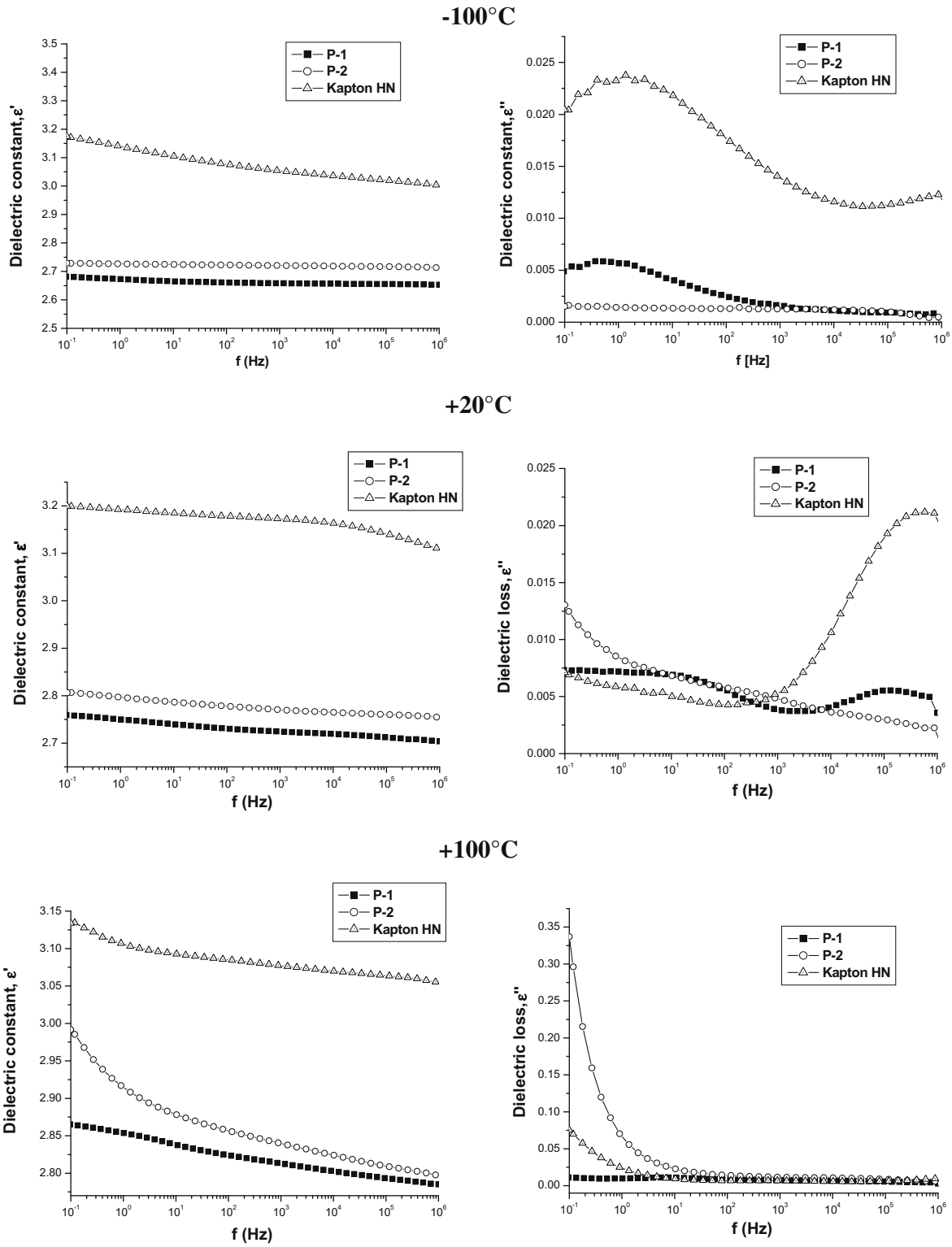

Fig. 2. Dependence of dielectric constant (ε') and dielectric loss (ε'') versus frequency, at three different temperatures.

rearrangements without disturbing the overall trajectory of the chain [35,36].

Characterization of the dynamic relaxation processes of polyimides as a function of constituent backbone structure

Table 2
Dielectric properties of siloxane-containing poly(oxadiazole-imide) films compared to **Kapton HN**® at selected frequencies and 23 °C.

Polymer	Dielectric constant, ε′				Dielectric loss, ε″			
	1 Hz	100 Hz	1 kHz	1 MHz	1 Hz	100 Hz	1 kHz	1 MHz
P-1	2.90	2.89	2.88	2.87	0.0059	0.0040	0.0034	0.0006
P-2	2.77	2.74	2.73	2.69	0.01	0.0071	0.0062	0.0078
Kapton HN®	3.24	3.22	3.19	3.13	0.006	0.0044	0.0049	0.02

has been an area of extensive activity. Dynamic mechanical and dielectric relaxation techniques have been widely applied to establish transition temperatures, relative relaxation intensity, and the time–temperature characteristics of the motional transitions encountered in these materials. Recently, a detailed report of the sub-glass and glass–rubber relaxation properties of Matrimid polyimide based on benzophenone-tetracarboxylic dianhydride and diaminophenylindane was reported [37]. A number of authors have summarized the common relaxation features of polyimides [38–40]. Typically, three relaxation processes are observed with increasing temperature, designated γ, β and α, respectively, with a corresponding to the glass–rubber relaxation. For Matrimid polyimide the peak temperatures corresponding to these relaxations are −112 °C (Tγ), 80 °C (Tβ) and 313 °C (Tα).

Here, the overall dynamic mechanical relaxation properties of the siloxane-containing polyimides **P-1** and **P-2**, in comparison with that of **Kapton HN**® were studied. The storage modulus (E'), the loss modulus (E'') and the loss factor ($\tan\delta$) versus temperature, at 1 Hz, are displayed from −150 to 500 °C in two separate figures: one for sub-glass transitions (Fig. 3) and another for α transition, at high temperature (Fig. 4).

The drops in E' curves and the peaks of E'' and $\tan\delta$ plots report on physical transitions in polymers. At very low temperatures, inferior to −125 °C (Fig. 3), **P-1** and **Kapton HN**® present high storage modulus values, over 10^9 Pa, which is typical for glassy polymers (−125 °C: $E'_{\mathbf{P\text{-}1}} = 3.7 \times 10^9$ Pa, $E'_{\mathbf{Kapton\ HN}^{®}} = 5.07 \times 10^9$ Pa). For **P-1** a barely perceptible decrease of E' starts around −100 °C that

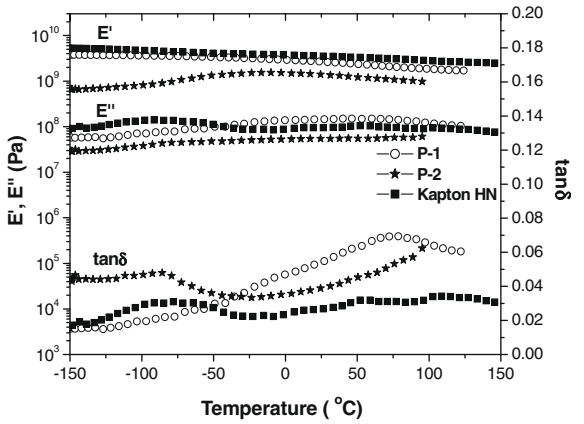

Fig. 3. DMA curves of **P-1**, **P-2** and **Kapton HN**® across the γ and β sub-glass transition region.

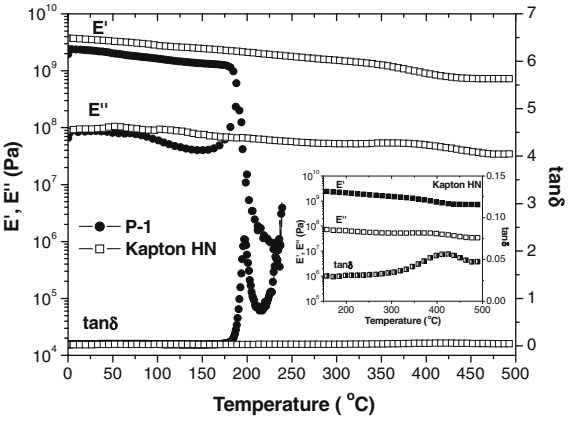

Fig. 4. DMA curves of **P-1** and **Kapton HN**® across the glass transition region (the inset illustrates more clearly the glass transition of **Kapton HN**® on DMA curves).

corresponds to extremely large peaks on E'' and tan δ plots. The tan δ peak is centred on 75 °C and E' decreases until 1.34×10^9 Pa at 150 °C. This peak could be associated with β transition. For the β transition in polyimides, various mechanisms have been postulated involving motions that, while still essentially local in character, encompass larger portions of the repeat unit that respond in a correlated manner. In more rigid systems, the origin of the β relaxation is linked to small amplitude motions that ultimately involve the entire repeat segment [41]. In the case of **P-1** this transition could be determined by local motions of diphenylether repeat units that respond in a correlated manner.

Unlike **P-1**, **Kapton HN**® film presents a γ transition centred on −80 °C on tan δ curve that can be associated with phenyl ring oscillations and is influenced by moisture absorption content, aging history and morphology which are absent in the polyimides **P-1** or **P-2** [38,42]. At higher temperatures, **Kapton HN**® displays two more secondary relaxations, β_1 and β_2, centred on 60 and 110 °C on tan δ curve [43]. The very small decrease of E' in this range (110 °C, $E'_{\mathbf{Kapton\ HN}^{®}} = 2.6 \times 10^9$ Pa) may be attributed to all these sub-glass transitions that are in progress. The **P-2** polyimide with *meta*-oriented ring has more flexible backbone and it is not surprising that the storage modulus at very low negative temperatures is under 10^9 Pa (−125 °C, $E'_{\mathbf{P\text{-}2}} = 0.71 \times 10^9$ Pa). A distinctive upturn in the E' modulus is displayed around −100 °C. Generally, an increase in E' with temperature in an isochronal DMA experiment, i.e. an increase of rigidity with rising temperature, may be assigned to three processes: crosslinking,

solvent evaporation and crystallization. Of these three alternatives crosslinking and solvent evaporation are not feasible over the temperature range in question. The raise of E' modulus is consistent solely with the evolution of a crystallization process. As far as we are aware, after a meticulous – but not exhaustive – survey of poly(imide siloxane) literature, the increase of the storage modulus in the negative temperature range was not reported. Some papers include the viscoelastic behaviour of poly(imide siloxane)s only in the positive temperature range [44,45]. However, the same trend of E' was found in the case of polyimide-polydimethylsiloxane copolymers containing nitrile groups, but no comments were made on it [46]. The *meta* orientation of phenyleneoxide aromatic rings and the presence of siloxane segments in the backbone impart a great mobility to **P-2** polyimide**.** Consequently, it becomes practicable the chain arrangement required for crystalline phase development. The small decrease of the storage modulus for **P-2** in the sub-glass transition range (-25 °C: $E' = 1.5 \times 10^9$ Pa; 100 °C: $E' = 0.95 \times 10^9$ Pa) reveals that it is a large and faint β relaxation for poly(siloxane-imide) with *meta*-catenation. Nevertheless, this β relaxation is overweighed by the orientation processes. Furthermore, passing onto the **P-2** high temperature behaviour (Fig. 4), the elevated flexibility of the polymer backbone affects the high temperature capabilities. The phenomena that accompany the glass transition are predominantly coordinated motions of polymer chain segments. It is not excluded that due to the very high flexibility of **P-2** polymer backbone, the raise of temperature induces motions of very large segments of chains or even coordinated movements of the whole polymer chain. On that account the slipping of the polymer chains past each other may take place. Maybe, this is why in the case of **P-2** the DMA experiment could not be conducted over 150 °C. The film has broken as it became softer, even though the experiment was repeated with or without the protection of the film clamping area in the tension attachment. The temperature range of glass transition overlaps the one of flowing and the determination of the glass transition by DMA is impeded.

The behaviour of **P-1** and **Kapton HN**® films in the high temperature range can be described comparatively (Fig. 4). The E' of **P-1** begins to turn down at 187 °C, this temperature being the onset of the glass transition. The tan δ peak, which is taken as the glass transition temperature, was found at 198 °C. In the glass transition range the storage modulus decreases till 1.6×10^6 Pa at 215 °C, i.e. it decreases three orders of magnitude. The variation of the dynamo-mechanical parameters with temperature is somehow different when the polyimide is **Kapton HN**®. The onset of the glass transition estimated as the fall of E' is around 335 °C and the peak of tan δ is centred on 420 °C. The fall of E' is very large spanning almost 100 degrees and the E' value at the end of this descent is 0.76×10^8 Pa. In the glass transition range the decrease of E' is less than one order of magnitude. It is well-known that for linear amorphous polymers the descent of E' in the glass transition range measures around three orders of magnitude and the behaviour of the **P-1** film is in agreement with this statement. The peculiarities of tan δ peak are meaningful to be examined. Fig. 4 displays for **Kapton HN**® a broad peak with an extremely low value of the peak amplitude (0.056), as opposed to the sharp and high peak (2.24) of **P-1**. The broadening of the transition is a sign for a large distribution of the relaxation times, which means a heterogeneous structure, whereas the amplitude of tan δ peak is related to the mobility of the polyimide backbone. The very low value of tan δ peak and the decrease of E' with less than one order of magnitude argue for the presence of strong constraints in **Kapton HN**®. Most probably they are represented by some degree of crosslinking formed during the preparation of the film or could be a result of the highly aromatic symmetrical character of this polyimide that leads to fairly stiff but extremely tough film [47].

Dielectric data for the γ and β transitions of siloxane-containing poly(oxadiazole-imide)s **P-1** and **P-2** in comparison with Kapton film are presented in Fig. 5.

Fig. 5 displays the dielectric constant and dielectric loss versus temperature in the frequency domain from 1 Hz to 10^6 Hz. The dielectric constant of the siloxane-containing polyimides **P-1** and **P-2** increases sharply with increasing temperature in a small range between 0.2 and 0.3 units. A step increase in the dielectric permittivity at the temperatures of the γ (**P-2** and **Kapton HN**®, 1 Hz) and β relaxations (**P-1** and **Kapton HN**®, 1 Hz**)** was observed. The segmental mobility allows for alignment of the dipoles, which results in an increase of the permittivity and causes the material to become less insulative. These step increases in the permittivity of **Kapton HN**® corresponding to γ and β relaxations are much larger than for siloxane-polyimides **P-1** and **P-2** indicating the presence of stronger dipoles in Kapton film.

The dielectric loss data also show distinct sub-glass transitions: peaks at ~110 °C for the β relaxation of **P-1** and ~60 °C for the β relaxation of **Kapton HN**®, and peaks at -85 °C for the γ relaxation of **P-2** and -90 °C for the γ relaxation of **Kapton HN**®, at 10 Hz (Fig. 6).

The plot showing the dependence of the dielectric loss (ε'') versus frequency for **P-1**, at -100 °C, displayed a peak corresponding to the γ relaxation of this polymer, even it was not evidenced in the dielectric loss (ε'') versus temperature plot. Probably, the γ and β relaxations are superposing, resulting in an extended transition over a large temperature domain.

Dielectric loss data (ε'') are compared with mechanical loss (E'') results across the sub-glass transition range in Fig. 7.

As compared with **Kapton HN**® film for which the position and breadth of each sub-glass relaxation in the dielectric spectra are in close correspondence with the dynamic mechanical curve, in the case of siloxane polyimide **P-1**, the position of β relaxation is shifted to higher temperature in dielectric loss curve (centred on 80 °C) compared with DMA curve (centred on ~50 °C). Moreover, based on the width and relative peak height of this sub-glass transition, the β process appears to be more prominent in the dynamic mechanical measurement. Such results from the DMA and broad-band dielectric spectroscopy (BDS) measurements indicate some degree of cooperative character inherent to the relaxation as detected by both techniques

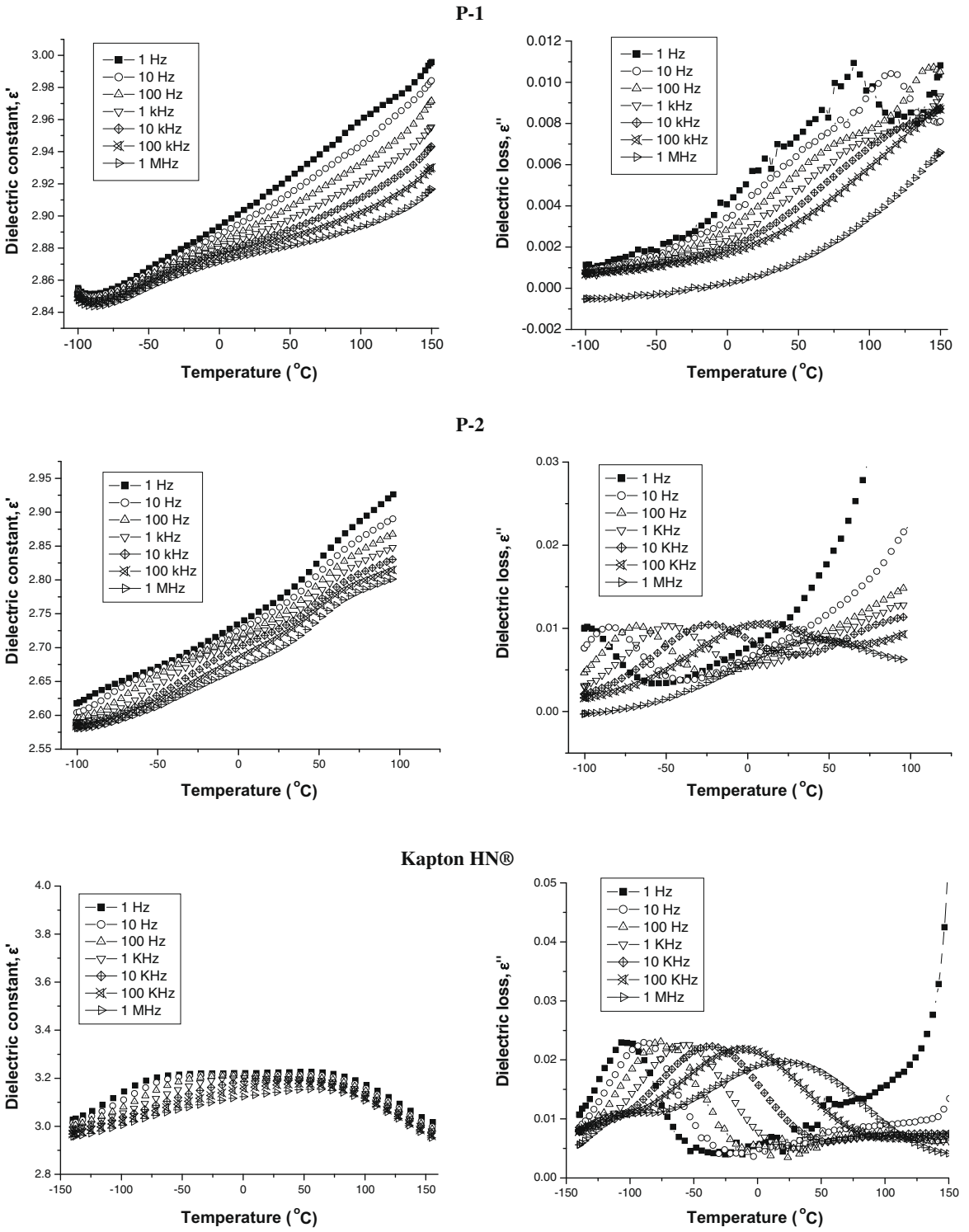

Fig. 5. Dielectric constant and dielectric loss versus temperature at various frequencies for **P-1**, **P-2** and **Kapton HN**® across the sub-glass transition region.

and suggest that the DMA measurement is capable of detecting a range of motions that encompass a higher level of cooperativity as compared to the dielectric probe. Considering the structure of the **P-1** molecule and the location of permanent dipoles within the repeat unit, one possible explanation for the contrasting dielectric and dynamic

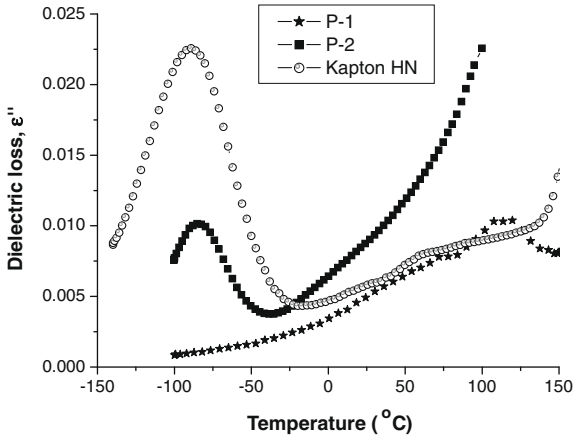

Fig. 6. γ and β Transitions observed for **P-1**, **P-2** and **Kapton HN**® in the dielectric loss versus temperature curves (frequency 10 Hz).

mechanical results is that the measured dielectric response is limited to motions of the oxadiazole diamine segment, while the dynamic mechanical response reflects longer-range correlated motions involving both portions of the repeat unit. The longer-range motions captured by the dynamic mechanical data would likely engender a higher degree of intra- and intermolecular cooperativity [37]. The γ relaxation of **P-1** observed in dielectric loss versus frequency curve at −100 °C was not clearly detected in DMA, or in the dielectric loss versus temperature curve. Also, the γ relaxation of **P-2** observed in dielectric loss versus temperature curve was not detected in the DMA curve. A possible explanation could be that this relaxation was superposing with the crystallization or rearrangement effect observed at the beginning, around −100 °C, in the DMA experiment. Such phenomena are not the case of detection by BDS; therefore the BDS displayed clear peaks on dielectric loss versus temperature attributed for γ relaxation of **P-2** polymer.

The molecular origins of the sub-T_g relaxations are clarified by using data from the BDS sub-glass transition relaxations in an Arrhenius activation energy analysis. The magnitude of the activation energy (*Ea*) of a relaxation depends on rotation potential energy barriers, internal friction, and the volume and environment of the moving repeat units. The activation energy of a relaxation calculated from dielectric data is generally lower than the activation energy calculated for the same relaxation from mechanical data [48]. The activation energy of γ and β relaxations of each polyimide was calculated by applying the Arrhenius equation:

$$f = A\exp(-Ea/RT)$$

where f is frequency, A is the pre-exponential factor, Ea is the activation energy, R is the gas constant, and T is the peak-maximum temperature. The activation energy for the γ relaxation of **P-1** was estimated from the dielectric loss versus frequency plots at −100, −95, −90 and −85 °C. The best-fit lines of the logarithmic frequency versus $1/T$ relationships distinguish the two types of relaxations.

The similarity in the activation energy for the γ relaxations suggests a common molecular origin. The γ relaxation *Ea* of 44 kJ/mol for **P-1**, 45 kJ/mol for **P-2** and 47 kJ/mol for **Kapton HN**® agrees reasonably well with the value of 43 kJ/mol reported for Matrimid polyimide [37]. Mechanical and dielectric activation energies for the β relaxation of aromatic polyimides have been reported in the range of 95–180 kJ/mol. The *Ea* values of the β relaxations are 107 kJ/mol for siloxane-containing polyimide **P-1** and 119 kJ/mol for **Kapton HN**®. Because the β relaxation maxima are very weak it is very difficult to determine their exact position and the error in calculation of the activation energy of this relaxation can be high. But if it takes into account the error in the activation energy calculation, the differences between the *Ea* for the β relaxation of our polymers and other polyimides that do not contains siloxane units, nor oxadiazole ring are not so high [49].

In order to analyze the conductivity relaxation of the polymer films, the complex permittivity is converted to the complex dielectric modulus $M^*(\omega)$. Considering the charges as the independent variable, conductivity relaxation effects can be suitably analyzed within the dielectric modulus formalism in terms of a dimensionless quantity, $M^*(\omega)$. Analogous to mechanical relaxation, the electric modulus $M^*(\omega)$ is obtained from the dielectric permittivity according to an equation described in the literature [50,51].

$$M^*(\omega) = 1/\varepsilon^*(\omega) = M' + iM''$$
$$= \varepsilon'/(\varepsilon'^2 + \varepsilon''^2) + i\varepsilon''/(\varepsilon'^2 + \varepsilon''^2)$$

The real and imaginary parts, M' and M'', respectively, of the dielectric modulus can be calculated from ε' and ε'':

$$M' = \varepsilon'/(\varepsilon'^2 + \varepsilon''^2)$$
$$M'' = \varepsilon''/(\varepsilon'^2 + \varepsilon''^2)$$

The main advantage of this formulation is that the space charge effects often do not mask the features of the spectra, owing to the suppression of high capacitance phenomena in M'' plots. The frequency dependencies of the real (M') and imaginary (M'') parts of the dielectric modulus for the polyimides **P-1**, **P-2** and **Kapton HN**® are shown in Fig. 8, as measured at three different temperatures.

The dispersions of M' and M'' indicate a presence of the distribution of conduction relaxation times. We can observe three relaxation processes taking place in **P-1** and **Kapton HN**® films. The first two, γ and β, are the secondary relaxations connected with local movements and they were also observed in the dependence of ε″ with frequency. The last one, taking place at high temperature, can be regarded as related to mobility of charge carriers and leading to system conductivity. This conductivity process masks the primary relaxation connected with glass transition and, partially the β relaxation process, also. The M'' spectra of these materials have a peak, and the frequency corresponding to it, known as relaxation frequency, f_M, is related to the ionic conductivity relaxation, where both charge carrier transport and reorientation may contribute to the electric field relaxation. When $f < f_M$, the charge carriers are mobile over long distances and are

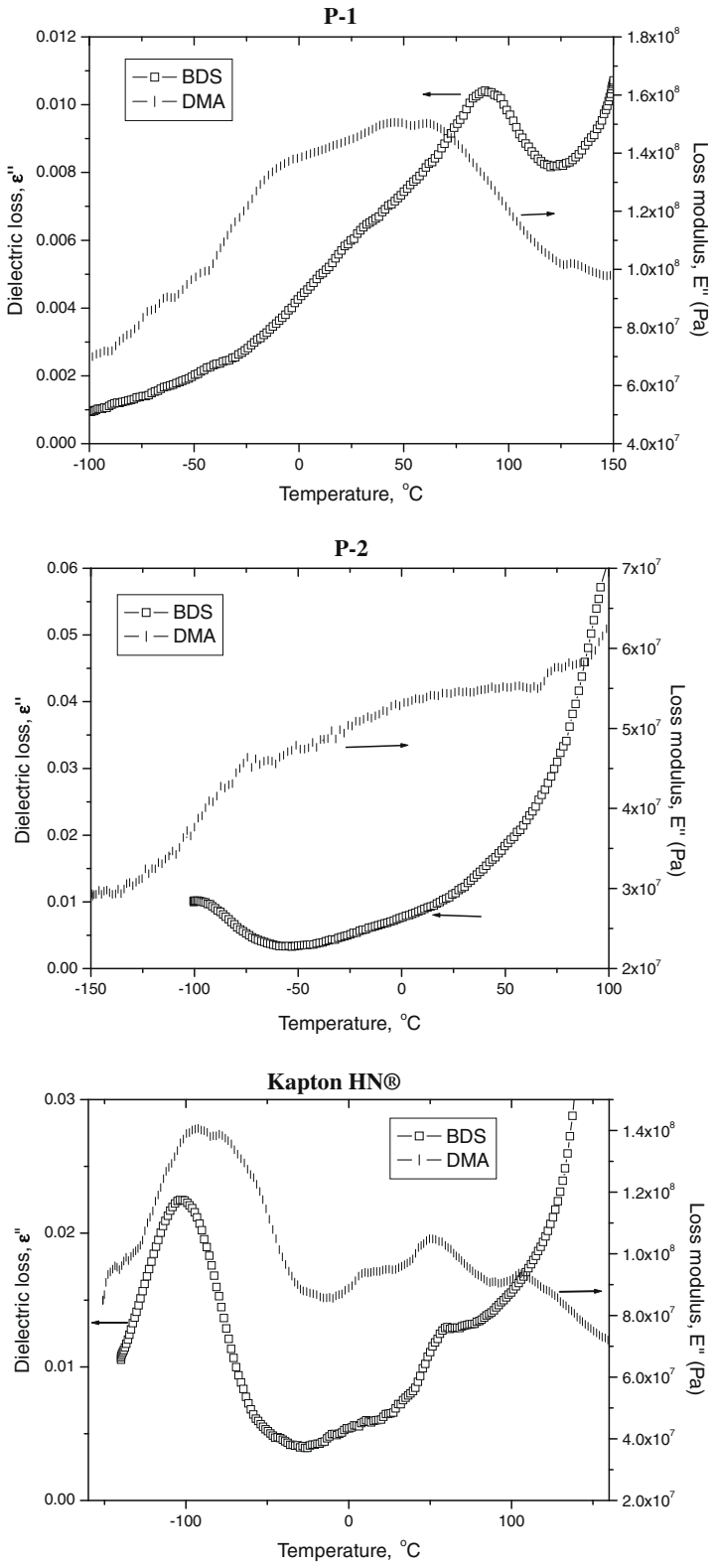

Fig. 7. Dynamo-mechanical loss modulus and dielectric loss versus temperature for **P-1**, **P-2** and **Kapton HN**® across the sub-glass transition region, at 1 Hz (DMA, dynamomechanical analysis, BDS, broadband dielectric spectroscopy).

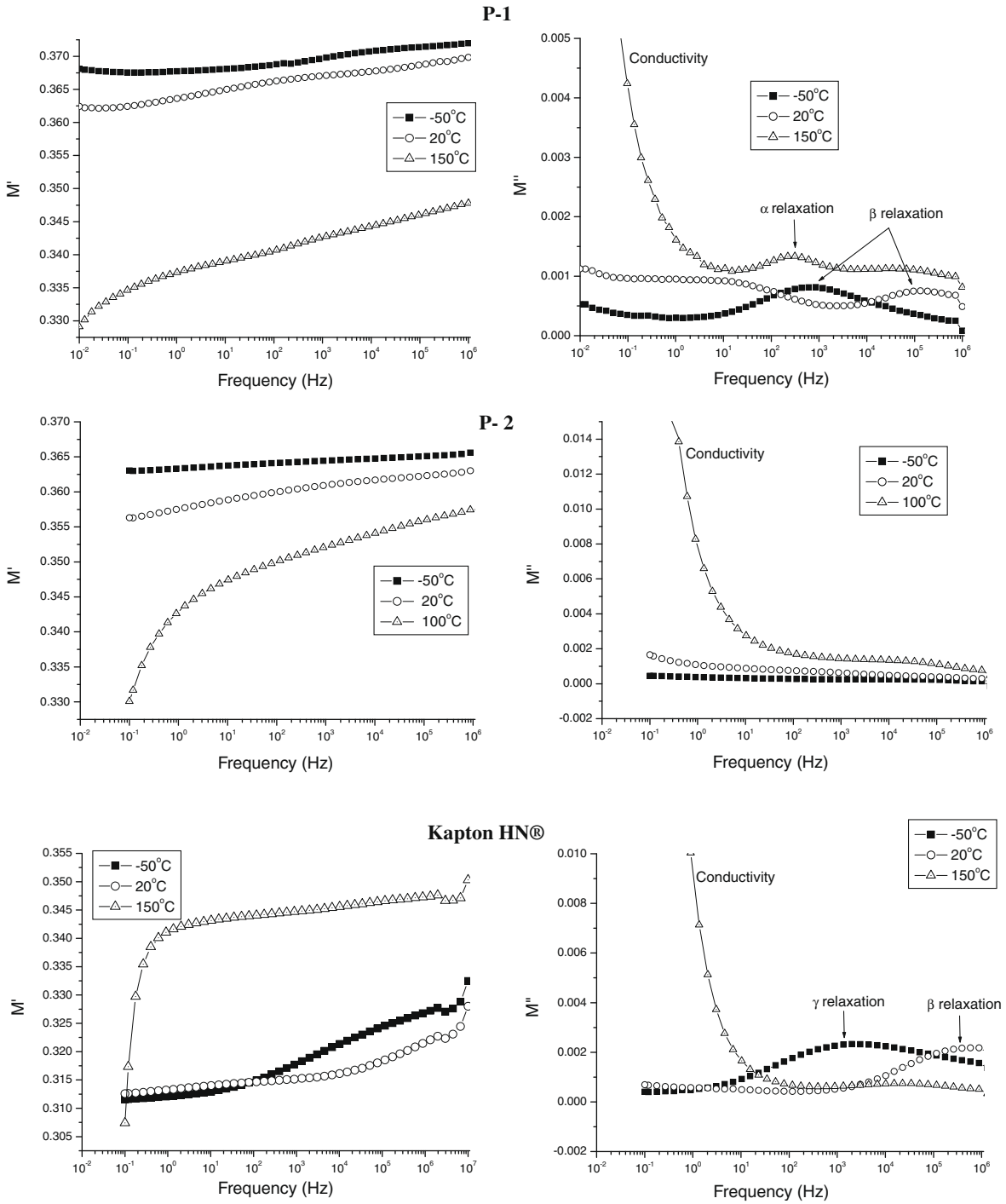

Fig. 8. Dielectric modulus and dielectric loss modulus versus frequency plots for **P-1**, **P-2** and **Kapton HN®** at different temperatures.

associated with the hopping conduction. For $f > f_M$, the carriers are spatially confined to their potential wells, being mobile over short distances and associated with the relaxation polarization processes. Thus, the peak frequency f_M is indicative of transition from long range to short range mobility [52,53].

4. Conclusions

Siloxane-containing poly(oxadiazole-imide)s were synthesized. Due to the bending of the chain as a result of the introduction of the siloxane group, the polymers were soluble in organic solvents thus being appropriate for processing

into transparent free-standing films from solutions, with good mechanical properties. The polymers had good thermal stability, their initial decomposition temperature being above 440 °C, and relatively low glass transition temperature. The dielectric constant values, measured at room temperature and in the frequency domain of 1 Hz–1 MHz, are in the range of 2.69–2.90, being significantly lower in comparison with that of **Kapton HN®** film. The dielectric loss values of the present polyimides are low, in the same range with that of **Kapton HN®**. The low values for both dielectric constant and dielectric loss indicate that the electrical signals loss will be lower in the dielectric medium. At low and moderate temperature, the polymer films studied by dielectric spectroscopy and dynamo-mechanical analysis showed γ and β relaxation processes connected with local movements of polymer chains. The dielectric properties corroborated with good mechanical behaviour and the very good film-forming ability make these polymers suitable for interlayer dielectric applications in microelectronics or in related fields.

References

[1] Wilson D, Stenzenberger HD, Hergenrother PM, editors. Polyimides. London: Blackie; 1990.
[2] Tummala RR, Keyes RW, Grobman WD, Kapur S. Thin film packaging. In: Tummala RR, Rymaszewski EJ, editors. New York: Van Nostrand Reinhold; 1989. p. 673–725.
[3] Ree M, Chen KJ, Kirby DP, Katzenellenbogen N, Grischkowsky D. Anisotropic properties of high-temperature polyimide thin films: dielectric and thermal-expansion behaviors. J Appl Phys 1992;72(5): 2014–22.
[4] Hougham G, Tesoro G, Viehbeck A, Chapple-Soko JD. Polarization effects of fluorine on the relative permittivity in polyimides. Macromolecules 1994;27(21):5964–71.
[5] DiMarzio EA, Gibbs JH. Glass temperature of copolymers. J Polym Sci 1959;40(136):121–31.
[6] Van Krevelen DW. Properties of polymers. 3rd ed. Amsterdam: Elsevier; 1990 [chapter 11].
[7] Leea YJ, Huang JM, Kuoa SW, Changa FC. Low-dielectric, nanoporous polyimide films prepared from PEO–POSS nanoparticles. Polymer 2005;46(23):10056–65.
[8] Maier G. Low dielectric constant polymers for microelectronics. Prog Polym Sci 2001;26(1):3–65.
[9] Rosenfeld J, Acharya HR, Choi JO, Suzuki T. In: Salamone JC, editor. Poly(imide siloxanes)s, vol. 8. Boca Raton: CRC Press; 1996. p. 6198–213.
[10] Furukawa N, Yamada Y, Furukawa M, Yuasa M, Kimura Y. Surface and morphological characterization of polysiloxane-*block*-polyimides. J Polym Sci A: Polym Chem 1997;35(11):2239–51.
[11] Mahoney CM, Gardella Jr JA, Rosenfeld JC. Synthesis and characterization of poly(imide-siloxane) copolymers containing two siloxane segment lengths: surface composition and its role in adhesion. Macromolecules 2002;35(13):5256–66.
[12] Schulz B, Brehmer L. In: Salamone JC, editor. Poly(arylene-1,3,4-oxadiazole)s, vol. 7. Boca Raton: CRC Press; 1996. p. 5595–604.
[13] Schulz B, Bruma M, Brehmer L. Aromatic poly(1,3,4-oxadiazole)s as advanced materials. Adv Mater 1997;9(8):601–13.
[14] Hamciuc E, Bruma M, Kopnick T, Kaminorz Y, Schulz B. Synthesis and study of new silicon-containing polyoxadiazoles. Polymer 2001; 42(5):1809–15.
[15] Thaemlitz CJ, Weikel WJ, Cassidy PE. Poly(oxadiazole-imide)s containing hexafluoroisopropylidene. Polymer 1992;33(15): 3278–85.
[16] Mercer FW. Synthesis and characterization of aromatic poly(ether ketone oxadiazole)s. High Perform Polym 1993;5(1):69–76.
[17] Hamciuc C, Hamciuc E, Ipate AM, Cristea M, Okrasa L. Thermal and electrical properties of copoly(1,3,4-oxadiazole-ethers) containing fluorene groups. J Appl Polym Sci 2009;113(1):381–3.
[18] Chen SH, Chen Y. Poly(*p*-phenylenevinylene) derivatives containing electron-transporting aromatic triazole or oxadiazole segments. Macromolecules 2005;38(1):53–60.
[19] Gomes D, Nunes SP, Pinto JC, Borges C. Synthesis and characterization of flexible polyoxadiazole films through cyclodehydration of polyhydrazides. Polymer 2003;44(13):3633–9.
[20] Souza FG, Sena ME, Soares BG. Thermally stable conducting composites based on a carbon black-filled polyoxadiazole matrix. J Appl Polym Sci 2004;93(4):1631–7.
[21] Hwang SW, Chen Y. Photoluminescent and electrochemical properties of novel poly(aryl ether)s with isolated hole-transporting carbazole and electron-transporting 1,3,4-oxadiazole fluorophores. Macromolecules 2002;35(14):5438–43.
[22] Wu TY, Sheu RB, Chen Y. Synthesis and optically acid-sensory and electrochemical properties of novel polyoxadiazole derivatives. Macromolecules 2004;37(3):725–33.
[23] Iosip MD, Bruma M, Robison J, Kaminorz Y, Schulz B. Study of related poly(1,3,4-oxadiazole-amide)s containing silicon or hexafluoroisopropylidene groups in the main chain. High Perform Polym 2001;13(3):133–48.
[24] Damaceanu MD, Bruma M. Study of fluorinated poly(1,3,4-oxadiazole-amide)s. Rev Roum Chim 2005;50(9–10):815–30.
[25] Damaceanu MD, Bacosca I, Bruma M, Robison J, Rusanov A. Heterocyclic polyimides containing siloxane groups in the main chain. Polym Int 2009;58(9):1041–50.
[26] Babu GN. In: Mittal KL, editor. Silicon-modified polyimides: synthesis and properties, vol. 1. New York: Plenum; 1984. p. 51–7.
[27] Hamciuc E, Hamciuc C, Cazacu M. Poly(1,3,4-oxadiazole-ether-imide)s and their polydimethylsiloxane-containing copolymers. Eur Polym J 2007;43(11):4739–49.
[28] Tan LS. In: Mark JE, editor. Poly(pyromellitimide-1,4-diphenyl ether). Oxford: Oxford University Press; 1999. p. 802–9.
[29] Hamciuc C, Hamciuc E, Bruma M, Klapper M, Pakula T. New aromatic poly(ether-ketone)s containing hexafluoroisopropylidene groups. Polym Bull 2001;47(1):1–8.
[30] Deligoz H, Yalcinyuva T, Ozgumus S, Yildirim S. Electrical properties of conventional polyimide films: effects of chemical structure and water. J Appl Polym Sci 2006;100(1):810–8.
[31] Hamciuc C, Hamciuc E, Ipate AM, Okrasa L. Copoly(1,3,4-oxadiazole-ether)s containing phthalide groups and thin films made therefrom. Polymer 2008;49(3):681–90.
[32] Xie K, Liu JG, Zhou HW, Zhang SY, He MH, Yang SY. Soluble fluoro-polyimides derived from 1,3-bis(4-amino-2-trifluoromethyl-phenoxy) benzene and dianhydrides. Polymer 2001;42(17): 7267–74.
[33] Hamciuc C, Hamciuc E, Pakula T, Okrasa L. Silicon-containing heterocyclic polymers and thin films made therefrom. J Appl Polym Sci 2006;102(3):3062–8.
[34] Sen S, Boyd RH. Dielectric relaxation in amorphous linear aliphatic copolyesters. Eur Polym J 2008;44(10):3280–7.
[35] Bravard SP, Boyd RH. Dielectric relaxation in amorphous poly(ethylene terephthalate) and poly(ethylene 2,6-naphthalene dicarboxylate) and their copolymers. Macromolecules 2003;36(3): 741–8.
[36] Jin W, Boyd RH. Time evolution of dynamic heterogeneity in a polymeric glass: a molecular dynamics simulation study. Polymer 2002;43(2):503–7.
[37] Comer AC, Kalika DS, Rowe BW, Freeman BD, Paul DR. Dynamic relaxation characteristics of Matrimid® polyimide. Polymer 2009;50(3):891–7.
[38] Habas JP, Peyrelasse J, Grenier-Loustalot MF. Rheological study of a high-performance polyimide. interpretation of the secondary mechanical relaxations of a nadimide crosslinked system. High Perform Polym 1996;8(4):515–32.
[39] Qu W, Ko TM, Vora RH, Chung TS. Effect of polyimides with different ratios of *para*- to *meta*- analogous fluorinated diamines on relaxation process. Polymer 2001;42(15):6393–401.
[40] Bas C, Tamagna C, Pascal T, Alberola ND. On the dynamic mechanical behavior of polyimides based on aromatic and alicyclic dianhydrides. Polym Eng Sci 2003;43(2):344–55.
[41] Ngai KL, Paluch M. Classification of secondary relaxation in glass-formers based on dynamic properties. J Chem Phys 2004;120(2): 857–73.
[42] Jonas A, Legras R. Relation between PEEK semicrystalline morphology and its subglass relaxations and glass transition. Macromolecules 1993;26(4):813–24.
[43] Kang PH, Jeon YK, Jeun JP, Shin JW, Nho YC. Effect of electron beam irradiation on polyimide film. J Ind Eng Chem 2008;14(5): 672–5.
[44] Ghosh A, Banerjee S. Synthesis, characterization, and comparison of properties of novel fluorinated poly(imide siloxane) copolymers. J Appl Polym Sci 2008;107(3):1831–41.

[45] Ghosh A, Banerjee S. Thermal, mechanical, and dielectric properties of novel fluorinated copoly(imide siloxane)s. J Appl Polym Sci 2008;109(4):2329–40.
[46] Hamciuc E, Hamciuc C, Cazacu M, Ignat M, Zarnescu G. Polyimide–polydimethylsiloxane copolymers containing nitrile groups. Eur Polym J 2009;45(1):182–90.
[47] Ambroski LE. H-film – a new high temperature dielectric. Ind Eng Chem Prod Res Dev 1963;2(3):189–94.
[48] Starkweather HW, Avakian P. Beta relaxations in phenylene polymers. Macromolecules 1989;22(10):4060–2.
[49] Eichstadt AE, Ward TC, Bagwell MD, Farr IV, Dunson DL, McGrath JE. Synthesis and characterization of amorphous partially aliphatic polyimide copolymers based on bisphenol-A dianhydride. Macromolecules 2002;35(20):7561–8.
[50] Macedo PB, Moynihan CT, Bose R. Role of ionic diffusion in polarization in vitreous ionic conductors. Phys Chem Glasses 1972;13(6):171–9.
[51] Sengwa RJ, Sankhla S. Characterization of ionic conduction and electrode polarization relaxation processes in ethylene glycol oligomers. Polym Bull 2008;60(5):689–700.
[52] Lanfredi S, Saia LS, Lebullenger R, Hernandes AC. Electric conductivity and relaxation in fluoride, fluorophosphate and phosphate glasses: analysis by impedance spectroscopy. Solids State Ionics 2002;146(3–4):329–39.
[53] Pal I, Agarwal A, Sanghi S, Sheoran A, Ahlawat N. Conductivity and dielectric relaxation in sodium borosulfate glasses. J Alloy Compd 2009;472(1–2):40–5.